TRANSITION NETWORK ENTROPY IN CHARACTERIZATION OF COMPLEXITY OF HEART RHYTHM AFTER HEART TRANSPLANTATION

Danuta Makowiec[b], Zbigniew R. Struzik[a,b], Beata Graff[c]
Marta Żarczyńska-Buchowiecka[c], Joanna Wdowczyk[c]

[a]Graduate School of Education, The University of Tokyo
RIKEN Brain Science Institute, Japan
[b]Institute of Theoretical Physics and Astrophysics, University of Gdańsk, Poland
[c]First Department of Cardiology, Medical University of Gdańsk, Poland

(Received February 24, 2014; revised version received June 4, 2014)

The transition network for *RR*-increments is a directed and weighted graph, where the vertices represent *RR*-increments and the edges correspond to subsequent increments. We show that based on the transition matrix of this network, the entropy of heart rhythm can be calculated. We compare the entropy of the distributions of eigenvalues of the transition matrix for heart transplant patients and for healthy young subjects. We show the regulatory effect of the autonomic nervous system on the entropy values and evaluate the effects of the progression of graft reinnervation on the entropy values.

DOI:10.5506/APhysPolB.45.1771
PACS numbers: 87.19.Hh, 87.18.–h

1. Introduction

It is generally believed that *RR*-intervals — time intervals between heart contractions — carry information about the cardiac control system, mainly driven by the autonomic nervous system [1]. Heart transplantation (HTX) interrupts the direct autonomic control over the beating of the heart. As a consequence, heart rate variability in patients after HTX is different from that of healthy people.

The decision to transplant the heart is taken when the patient's life is in danger, and HTX is generally seen as a life saving operation. In many cases, already in a short time after the surgery, it is amazing to see how the organism of the patient recovers [2].

Therefore, when we investigate signals recorded from the same patient with the passing of time after HTX, we have a unique opportunity to observe the heart at work when the direct control over healthy variability is removed and subsequently recovers, at least partially.

RR-signals, like any time series, can be mapped into a directed graph where the vertices represent signal values and the edges are links between consecutive values in a signal [3, 4]. A variety of measures have been proposed to determine the relative importance of a single vertex within the graph and to quantify the topology of vertex connectivity [5, 6]. Examples of such measures are given by the centrality degree defined as the degree of a vertex or the transition matrix which introduces the probabilistic description of the dynamical aspect of the network topology. The considerable success of the network approach motivated us to explore these ideas to identify patterns in *RR*-signals of people after HTX, and present them in a way which could be useful in clinical practice to observe the progress of reinnervation and the restoration of the function of autonomic regulation.

This paper is a continuation of our earlier investigations (see [7–10]). Previously, we studied the emergence of complexity in transition networks constructed from *RR*-series [7, 8], and from increments between subsequent *RR*-intervals [9, 10]. In [9] we further studied networks representing fluctuations in the heart *RR*-intervals, and not the actual intervals. There, we investigated disintegration of such networks by measuring changes in the volume of the network remaining after subsequent removal of vertices which described events with a given increasing probability. Then, in [10] we proposed assessment of the complexity of heart *RR*-interval variability by means of calculating the entropy of the transition matrices of those networks.

In the following, we investigate properties of the dynamical topological description of time series using the transition matrix approach to cardiac signals obtained from healthy young people and people after HTX. These results are then compared with transition networks obtained from Fourier phase surrogates to measure the influence of the higher order, non-linear correlations in the data. In order to assess the complexity of the signals studied, we formulate the description of the topology using entropy. We observe that the entropy measure applied captures the fine change in non-linear topological properties of the time series transition matrix. In particular, we reveal a systematic change in complexity occurring during graft adaptation and the reinnervation progress in HTX subjects.

2. Data acquisition

2.1. Groups of signals studied

We study two groups of signals: Young and HTX. The Young group consists of 41 recordings (21 women and 20 men, age 19–34) which were obtained from healthy young people — students of Gdańsk Medical University. The HTX group is made of 25 recordings taken from 16 patients after HTX. The information about the age and sex of each patient is given in Fig. 7. All the patients had had the HTX at least 12 months previously and qualified as healthy. Some recordings were taken from the same patients but at different periods after the surgery which allows the study of the progress in graft adaptation. Among the 25 signals from the HTX group, five of the signals are special because they come from patients who suffered from graft rejection not less than five months later or not less than six months previously.

All the subjects underwent full twenty-four-hour Holter monitoring, during a normal sleep–wake rhythm. The Holter recordings were analyzed by Del Mar Reynolds Impresario software and screened for premature, supraventricular and ventricular beats, missed beats and pauses. Finally, the signals were manually surveyed and annotated.

2.2. Signal preprocessing

Our Holter equipment provided values with 128 Hz sampling frequency. Therefore, the *RR*-intervals are given with 7.8125 msec. resolution, which can be approximated by $\Delta_0 = 8$ msec. For this reason, *RR*-interval signals take values which are multiples of 8.

The nocturnal period of the circadian rhythm is known to be a dynamic state which is characterized by rapid fluctuations in the activity of the autonomic nervous system controlling the coronary artery, systemic blood pressure, and heart rate [11]. As a consequence, the heart rate variability is typically higher during the night-time. Moreover, the nocturnal regulation of the heart contractions is evidenced as the most free from influences of types other than the autonomic nervous system regulation. Based on these facts, our analysis was focused on sleeping hours, namely the *RR*-intervals were extracted from 24:00 to 04:00 in the case of signals from the Young group and from 22:00 to 06:00 in the case of signals from the HTX group.

To ensure well founded statistics for the analysis, the series were constructed from a total of 15 000 normal-to-normal *RR*-intervals. We considered continuous data segments consisting of at least 500 consecutive normal-to-normal heart contractions, excluding ectopic beats and any other data corruption or noise. On average a signal from the Young group consisted of 5.17 ± 1.05(95% C.I.) such segments of continuous *RR*-interval data, while

a signal from the HTX group contained 7.50 ± 1.56(95% C.I.) segments, see Fig. 1 for a more detailed description of the data segment statistics. In the analysis, we omitted any information from neighbouring samples across adjacent data segments.

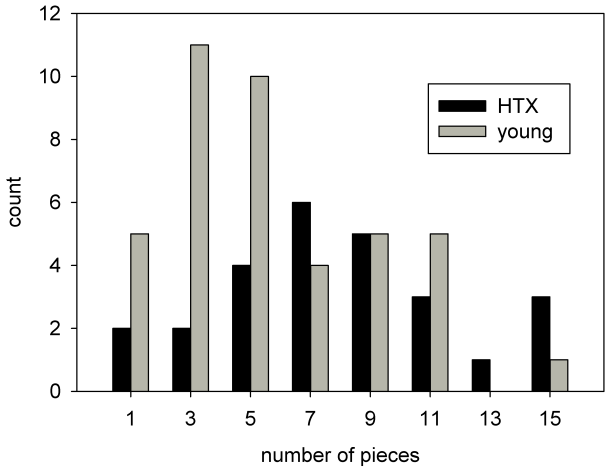

Fig. 1. Histogram of events of the number of ECG recording segments from which a given signal was constructed.

RR-increments, *i.e.*, differences between subsequent RR-intervals: $\Delta RR(t) = RR(t) - RR(t-1)$, are also multiples of 8, with values limited to $0, \pm 8, \pm 16, \pm 24, \ldots$ Here negative values of RR-increments correspond to events of accelerations, while positive values denote decelerations, and 0 describes a so-called no-change event.

We applied a standard binning procedure, using bins based on multiples of the signal resolution, namely $\Delta = k\Delta_0$ for $k = 1, 2, \ldots$ This decreases the number of different values appearing in a sequence of RR-intervals, and, in consequence, decreases the number of distinct vertices in the transition network obtained for RR-intervals.

In addition, we performed the same analysis on artificially modified cardiac signals, which we refer to as surrogate signals, obtained by randomization of phases of the Fourier transform of the cardiac RR-intervals (note, not RR-increments). Such surrogate signals preserve the linear correlations of the cardiac signals [12] and therefore they can be used to detect nonlinearity in the original data. The surrogate signals were prepared with the help of the TISEAN software [13]. For each cardiac signal we prepared ten surrogate signals. Each signal was analyzed independently and then the group average was calculated.

3. Transition network for *RR*-increments

Let $\boldsymbol{b} = \{b_0, b_2, \ldots, b_i, \ldots, b_N\}$ be a sequence of *RR*-intervals binned with some Δ. The subscript i refers to the time order. Further, let $\boldsymbol{c} = \{c_1, c_2, \ldots, c_i, \ldots, c_N\}$ be a sequence of the corresponding *RR*-increments, *i.e.*, $c_i = b_i - b_{i-1}$. Since the number of different values is finite, let us denote it as K. We can order the values from the smallest $C^{\min} = \min_i\{c_1, c_2, \ldots c_N\}$ to the greatest $C^{\max} = \max_i\{c_1, c_2, \ldots c_N\}$, and use them as labels for the vertices of the network:

$$\begin{aligned} C^{\min} &= C^{(1)}, \qquad C^{(2)} = C^{(1)} + \Delta, \ldots, \\ C^{\max} &= C^{(K)} = C^{(1)} + (K-1)\Delta. \end{aligned} \tag{1}$$

A directed edge $(C^{(I)}, C^{(J)})$ between two vertices $C^{(I)}$ and $C^{(J)}$ is drawn, if $C^{(I)}$ and $C^{(J)}$ represent a pair of consecutive events in a sequence $\boldsymbol{c}$, namely $(c_i = C^{(I)}, c_{i+1} = C^{(J)})$. If a given pair occurs many times in $\boldsymbol{c}$, then the weight of the corresponding edge increases to reflect the counts of occurrences. The loops, if they appear, denote consecutive decelerations or accelerations of the same size. The loop accompanying vertex 0 demonstrates the presence of two consecutive no-change events.

We construct a matrix of transitions between the states represented by the network. The so-called 'transition matrix' T of a $K \times K$ size is defined as follows. Each element $T_{(I)(J)} = T(C^{(J)}|C^{(I)})$ equals:

1. the weight of the outgoing edge from vertex $C^{(I)}$ to vertex $C^{(J)}$, normalized by the total weight of the vertex $C^{(I)}$, or

2. zero if there is no edge between these vertices.

The resulting matrix $\boldsymbol{T}$ describes the probability of transitions between two states given that the $C^{(I)}$ state occurs. The edges follow a natural order in the time series and each outgoing edge is accompanied by an incoming edge. As a consequence, the total transition probability of the outgoing edges is equal to the sum the transition probabilities of the incoming edges, and matches a given *RR*-increment occurrence of a signal.

In other words, the transition matrix describes a Markov walk on a network where a walker moves from the vertex $C^{(I)}$ to $C^{(J)}$ with a probability $T_{(I)(J)}$. Consequently, matrix $\boldsymbol{T}$ is right stochastic.

The role of vertices in the network can be inferred from the stationary distribution arising from the transition matrix $\boldsymbol{T}$. The stationary state $\mu = \{\mu_{(I)} : (I) = C^{\min}, \ldots, C^{\max}\}$ is given as the eigenvector of the transition matrix $\boldsymbol{T}$ corresponding to eigenvalue 1. Consequently, we can calculate the

entropy as follows

$$S = -\sum_{(I)=1}^{K} \mu_{(I)} \sum_{(J)=1}^{K} T_{(I)(J)} \log T_{(I)(J)} \,. \tag{2}$$

4. Results

Directly after the HTX, the RR-signals of the patients are very plain. The absence of any influence of the autonomic nervous system results in very low variability of RR intervals. As a result of this, the network representation of RR-increments consists of considerably fewer vertices than for a typical healthy person. We illustrate this by presenting the values of the mean transition matrices found for the Young subjects and HTX patients. These mean matrices are found after averaging transition matrices obtained for the individual patients from each of the three groups considered: Young, HTX and Surrogates. In Fig. 2 we show them as density plots.

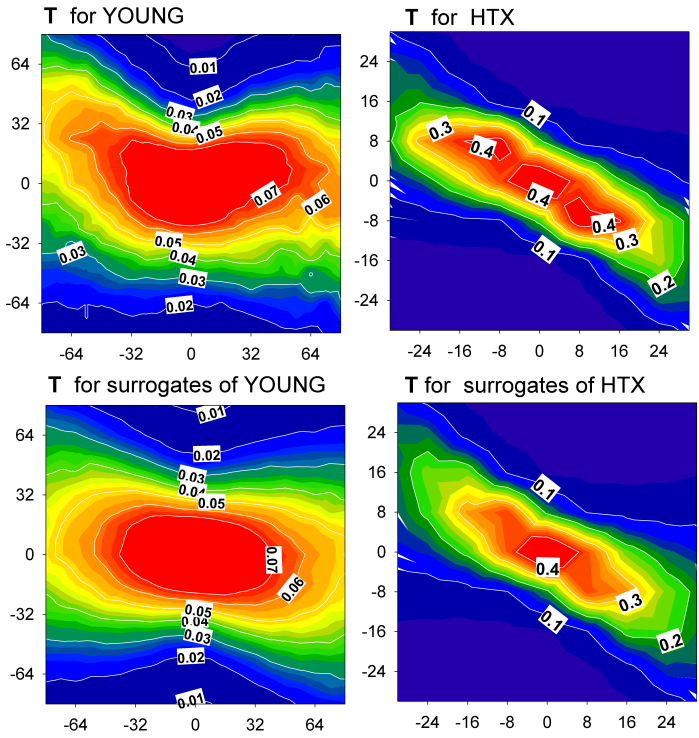

Fig. 2. Density plots for mean transition matrices obtained from RR-increments for the main cardiac groups: Young and HTX at the signal resolution, *i.e.*, $\Delta = 8$ msec. Note the difference between the scales used in the plots.

From Fig. 2 we see that the network constructed from signals of HTX patients is concentrated around the transition from a no-change event to the smallest increments possible, namely $0, \pm 8, \pm 16$. The plots obtained from surrogate signals indicate that nonlinear effects are related to events distant from the event of the no-change-to-no-change type.

In Fig. 3 we show two networks constructed from the means of events obtained from signals of HTX recipients and Young people. Events which occur with a probability of less than 1% are omitted. Both networks consist of 7 events only. Each vertex is connected to all others. The probability of the particular transition is represented by the edge width. Both networks appear to have a similar topology. The most popular transition is $(0; 0)$, namely transition from no-change to no-change. However, each network describes events at a different scale.

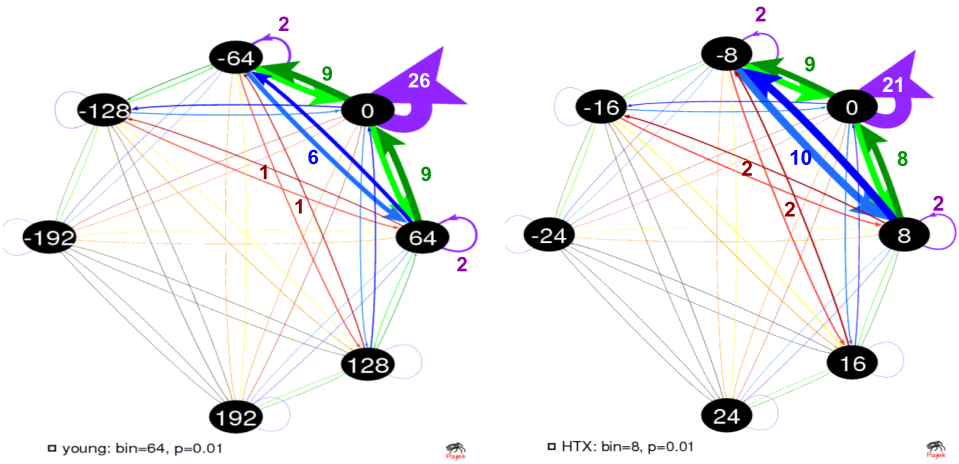

Fig. 3. (Colour online) The mean networks for the Young (left) and HTX (right) groups with counts for the important transitions in per cents. Veritices are arranged in a circle and ordered clockwise according to the label value. Note that the HTX signals are binned at $\Delta = 8$ msec., while the Young group signals are binned of $\Delta = 64$ msec. The edge width mimics counts for the given transitions. The edge label indicates the probability that a given pair of increments occur subsequently in a signal. The following colour scheme is applied for edges to reveal changes between subsequent transitions: no-change: violet loops; Δ-change: green edges for nearest neighbours of the circle; 2Δ-change: blue edges for next-nearest neighbors; 3Δ-change: red edges for next-nest-neighbors; 4Δ-change: yellow egdes if vertices representing transitions are separated by three other vertices and other cases are represented by black edges. The diagrams were prepared with the use of Pajek [14].

In Fig. 4 we specify the differences in the dynamics between HTX patients and Young people by showing the density plots of differences between the corresponding transition matrices. These differences are shown when the same scale to quantify events is applied to both groups, and when the events occurring in the Young group are represented at a scale 8 times greater than events in signals from the HTX group. The networks in Fig. 3 likewise reveal differences using these scales. In particular, we see that:

— $T_{\mathrm{HTX}}(0|0) \approx T_{\mathrm{Young}}(0|0)$ when 0 denotes a change within less than 8 msec in the case of HTX patients and within less than 64 msec in the case of Young people;

— $T_{\mathrm{HTX}}((n*8)|(-m*8)) > T_{\mathrm{Young}}((n*64)|(-m*64))$ and $T_{\mathrm{HTX}}((-n*8)|(m*8)) > T_{\mathrm{Young}}((-n*64)|(m*64))$ for $n < m : 1, 2, 3, 4$ which quantifies the following transitions: *(i)* after a given acceleration, the correcting deceleration occurs, or *(ii)* after a given deceleration, the acceleration occurs;

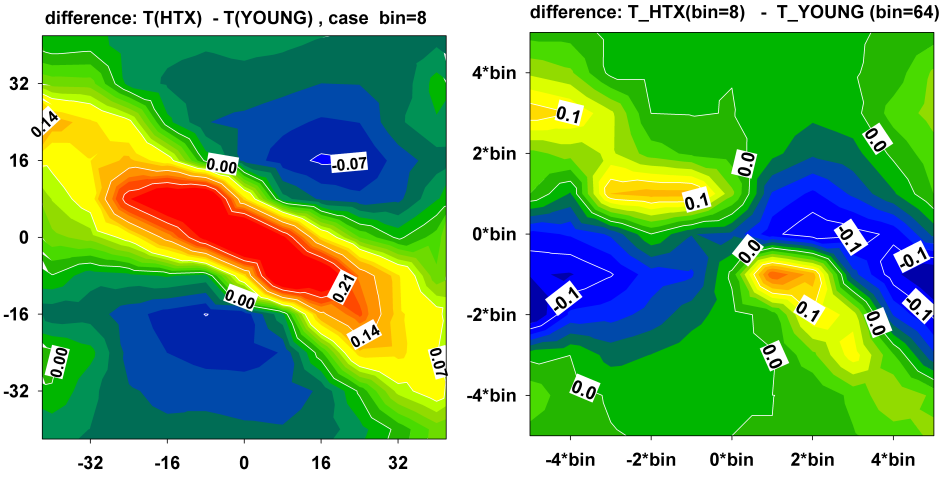

Fig. 4. (Colour online) Density plots of differences between the considered transition matrices when both matrices are represented with the same bin, bin = 8 [msec] (left) and when the bin for the Young group is 8 times greater (right). The regions close to lines labeled 0.0 (plotted in green) represent transitions which occur with a similar probability in both groups. Lines with positive labels mark regions of transitions which are more popular in signals of HTX patients. These regions are filled by the yellow and red colours. Lines with negative labels delimit regions which are specific to signals from of Young people. They are drawn in blue. Note that the labels used in the right figure are for HTX, and in the case of the Young, they have to be multiplied by 8.

— $T_{\mathrm{HTX}}((-n*8)|(-m*8)) < T_{\mathrm{Young}}((-n*64)|(-m*64))$ and $T_{\mathrm{HTX}}((n*8)|(m*8)) < T_{\mathrm{Young}}((n*64)|(m*64))$ for $n < m : 1, 2, 3, 4$, *i.e.*, two accelerations, and two decelerations occur in a sequence.

Now, let us discuss the differences between the types of signals: cardiac *versus* surrogate by using the properties of stationary measures arising from the mean transition matrices. In Fig. 5 stationary measures obtained for the Young and HTX groups are shown, together with stationary measures of their respective Surrogates.

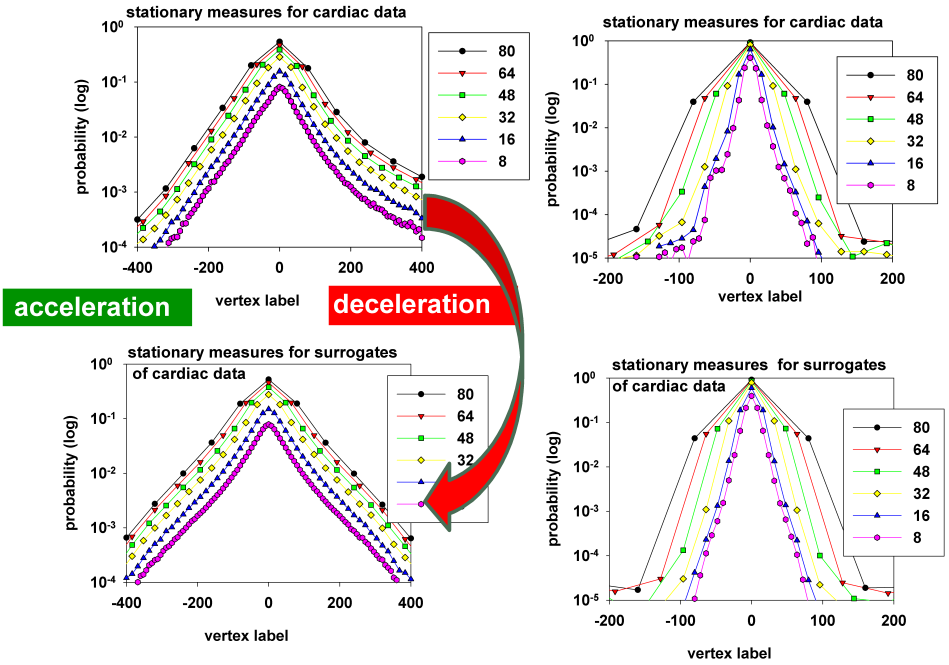

Fig. 5. Plots of eigenvectors for the eigenvalue 1 of the mean transition matrices obtained for cardiac and surrogates signals when data is binned with different bin sizes Δ (log-plots), and for the Young group (left panel) and the HTX group (right panel.)

One should note that the binning procedure does not change the importance of vertices. For each group studied, the main measure is associated with no-change transitions. But while in the case of the Young group the probability of the no-change-to-no-change event takes values from 0.08, for $\Delta = 8$, to 0.47 for $\Delta = 80$, for signals from the HTX group we obtain 0.41 and 0.92, respectively. The Surrogate data provide similar characteristics for the main transitions. However, one can see discrepancies when decelerations are large, namely for RR-increment > 150 msec.

The entropy values at the maximal resolution Δ_0 are as follows:

	Cardiac	Surrogates
Young	1.46	1.49
HTX	0.58	0.63

and, as expected, they decrease with the increasing bin, as is shown in Fig. 6. However, in each other bin, the entropy estimated from the surrogates is still larger than the entropy obtained from the cardiac signals.

It should be noted that the values presented are slightly different from those in [10]. Here, the entropy is calculated from the mean transition matrix while previously the entropy was estimated as the mean of the entropies calculated for each individual signal.

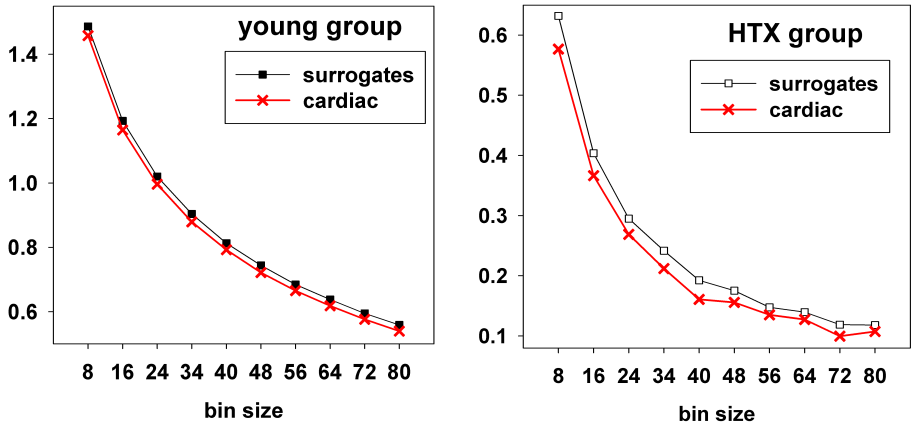

Fig. 6. Entropy calculated from the mean transition matrices obtained for the Young (left) and HTX (right) groups when individual signals are binned with different bin size.

The small relative difference between entropies found for cardiac and surrogate signals of the Young group lead to the observation that changes in RR-intervals follow linear stochastic dynamics.

This relative difference is greater in the case of HTX signals. Hence, we can hypothesize that the rhythm of the heart in patients after a HTX is driven by nonlinear interactions to a greater degree than in healthy individuals. Furthermore, we can attribute the stochastic linearity of healthy dynamics to the direct influence of the autonomic nervous system.

Finally, let us observe whether the entropy changes as time passes after the surgery. In Fig. 7 we show the entropy calculated for each individual HTX patient with indications of the time after HTX. The entropy increases

in most cases, consistently with the length of time after the heart transplantation, as is represented in the right panel of Fig. 7, in spite of considerable variability. This, in our opinion, reflects the progression of restoration of the dynamics in the heart rate variability of the patients as a result of increased cardiac control by the autonomic system. Moreover, it can also be observe that the entropy calculated from signals of three of the five patients in whom the graft rejection episode had been/was to be observed are far from the mean value for the group.

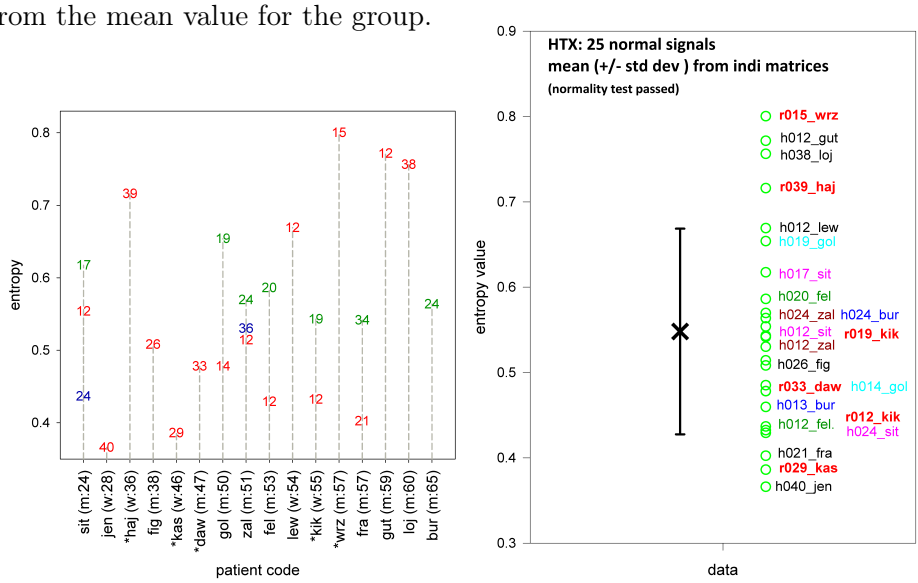

Fig. 7. Entropy calculated for 25 signals from 16 patients in the HTX group. Left: Symbolic patient codes are listed along the horizontal axis. In brackets, the sex and the age at the time of surgery are given. Codes starting with a ∗ mark patients qualified as healthy, but for whom the rejection episode had been/was to be recorded. For a given patient, the values of entropy are marked by indicating numbers of months after the surgery. Right: The same set of entropy values displayed with respect to the mean value obtained for the HTX group. The letters 'h' and 'r' in the labels are used to code the clinical information about whether the symptoms for rejection of the graft would develop 'r' or not 'h' in the future/had developed in the patient's history. The numbers in the labels correspond to the time after the surgery (in months). The postfixes identify the patients as they are identified in the left panel.

The possibility of a reliable evaluation of the restoration of the dynamics of cardiac variability would be of paramount significance in the evaluation of graft adaptation and the general restoration of a patient's circulatory dynamics. However, the sample size in our study is much too small to permit the formulation of any definitive conclusions.

5. Conclusions

HTX is a costly and extreme life saving intervention which restores the blood circulatory function, but depraves the system of the patient of the autonomic control and the related dynamical responsiveness of the heart. In evaluating the progression of the graft adaptation into the system and partial restoration of the autonomic regulation through reinnervation, the evaluation of the dynamical properties of the heart rate variability is considered to provide valuable insight. We have verified that entropy values capture the complex dynamical properties of the heart rate variability dynamics and may in the future help to evaluate the progression of the reinnervation process and related restoration of the HRV dynamics.

We thank the Polish National Science Centre for financial support: UMO:2012/06/M/ST2/00480.

REFERENCES

[1] M. Malik *et al.*, *Eur. Heart J.* **17**, 354 (1996).
[2] R. Toledo *et al.*, *Am. J. Physiol. Reg. Int. Comp. Physiol.* **282**, R900 (2002).
[3] R.V. Donner *et al.*, *New J. Phys.* **12**, 033025 (2010).
[4] A.S.L.O. Campanharo *et al.*, *PLoS ONE* **6**, e233378 (2011).
[5] M.E.J. Newman, *Phys. Rev.* **E74**, 036104 (2006); M.E.J. Newman, *The Mathematics of Networks*, in: *The New Palgrave Encyclopedia of Economics*, 2nd edition, L.E. Blume, S.N. Durlauf (eds.), Palgrave Macmillan, Basingstoke 2008.
[6] L. da F. Costa, F.A. Rodrigues, G. Travieso, P.R. Villas Boas, *Adv. Phys.* **56**, 167 (2007).
[7] D. Makowiec *et al.*, *Acta Phys. Pol. B Proc. Suppl.* **4**, 139 (2011).
[8] D. Makowiec *et al.*, in: Proceedings of the 7th ESGCO 2012, Kazimierz Dolny, Poland, 2012.
[9] D. Makowiec *et al.*, *Acta Phys. Pol. B* **44**, 1219 (2013).
[10] D. Makowiec *et al.*, in: Proceedings of Engineering in Medicine and Biology Society (EMBC), 2013 35th Annul International Conference on the IEEE, 6127, 2013.
[11] E. Vanoli *et al.*, *Circulation* **91**, 1918 (1995).
[12] T. Schreiber, A. Schmitz, *Physica D* **142**, 346 (2000).
[13] R. Hegger, H. Kantz, T. Schreiber, *Chaos* **9**, 413 (1999) with TISEAN software accessible from `http://www.mpipks-dresden.mpg.de/~tisean/Tisean_3.0.1`
[14] V. Batagelj, A. Mrvar, Pajek 1.26, accessible from `http://pajek.imfm.si/doku.php?id=download`